B7-H3 Specific CAR T Cells for the Naturally Occurring, Spontaneous Canine Sarcoma Model

Shihong Zhang[1], R. Graeme Black[1], Karan Kohli[1], Brian J. Hayes[1], Cassandra Miller[2], Amanda Koehne[1], Brett A. Schroeder[1,3], Kraig Abrams[1], Brian C. Schulte[4], Borislav A. Alexiev[5], Amy B. Heimberger[6], Ali Zhang[7], Weiqing Jing[7], Juliana Chi Kei Ng[7], Himaly Shinglot[7], Bernard Seguin[8], Alexander I. Salter[1], Stanley R. Riddell[1,9], Michael C. Jensen[10], Stephen Gottschalk[11], Peter F. Moore[12], Beverly Torok-Storb[1], and Seth M. Pollack[1,7]

ABSTRACT

One obstacle for human solid tumor immunotherapy research is the lack of clinically relevant animal models. In this study, we sought to establish a chimeric antigen receptor (CAR) T-cell treatment model for naturally occurring canine sarcomas as a model for human CAR T-cell therapy.

Canine CARs specific for B7-H3 were constructed using a single-chain variable fragment derived from the human B7-H3–specific antibody MGA271, which we confirmed to be cross-reactive with canine B7-H3. After refining activation, transduction, and expansion methods, we confirmed target killing in a tumor spheroid three-dimensional assay. We designed a B7-H3 canine CAR T-cell and achieved consistently high levels of transduction efficacy, expansion, and *in vitro* tumor killing. Safety of the CAR T cells were confirmed in two purposely bred healthy canine subjects following lymphodepletion by cyclophosphamide and fludarabine. Immune response, clinical parameters, and manifestation were closely monitored after treatments and were shown to resemble that of humans. No severe adverse events were observed.

In summary, we demonstrated that similar to human cancers, B7-H3 can serve as a target for canine solid tumors. We successfully generated highly functional canine B7-H3–specific CAR T-cell products using a production protocol that closely models human CAR T-cell production procedure. The treatment regimen that we designed was confirmed to be safe *in vivo*. Our research provides a promising direction to establish *in vitro* and *in vivo* models for immunotherapy for canine and human solid tumor treatment.

Introduction

Chimeric antigen receptor (CAR) T-cell therapies have transformed the care of patients with lymphoid malignancies. For the treatment of solid tumors, CARs targeting GD2, HER2, EGFR, mesothelin, and other cell surface proteins are under development (1). Although CAR T cells demonstrated potentials in solid tumor applications, there are several significant challenges, including trafficking of infused lymphocytes into the tumor microenvironment, overcoming immune checkpoints and regulatory immune infiltrates, which must be accomplished while maximizing T-cell persistence yet minimizing toxicity (2, 3). Furthermore, because the targets for solid tumor for the most part are self-antigens, the safety of some CAR T-cell targets remains a concern (4, 5). These challenges can only be partially studied in mouse models due to the drastic difference in immune and tumor microenvironment components. Successful treatments in mouse models rarely directly translate into effective human cancer control. This is particularly true for solid tumor immunotherapy where immune incompetent models may lack functional elements of the tumor immune microenvironment that are critically important. Therefore, testing different treatment plans in an immunocompetent model with naturally occurring tumors may help bridge the gap between novel immunotherapies and effectiveness.

Naturally occurring canine cancers are in many ways highly comparable with human cancers and can serve as a model for human solid tumor immunotherapy. Gene expression pattern of canine osteosarcoma was found to be indistinguishable from human osteosarcoma (6). Whole-genome sequencing and whole-exome sequencing of canine osteosarcoma also revealed that similar to human osteosarcoma, canine osteosarcoma has low mutational burden, low immune cell infiltration, and similar tumor-driving mutations (7). Other types of tumors including melanoma, mammary tumor, and soft-tissue sarcoma (STS) also show high levels of similarity between canine and the human counterparts (8). In addition, some relatively rare human cancers are common in dogs. While less than 1,000 cases of human osteosarcoma are diagnosed in the United States annually, approximately 10,000 to 45,000 cases of canine osteosarcoma are diagnosed each year (9). Canine lymphoma subtypes, STS, and skin cancers are also more prevalent than their human counterparts (8). These high

[1]Clinical Research Division, Fred Hutchinson Cancer Research Center, Seattle, Washington. [2]Comparative Medicine, Fred Hutchinson Cancer Research Center, Seattle, Washington. [3]NCI, NIH, Bethesda, Maryland. [4]Department of Medicine, University of California San Francisco, San Francisco, California. [5]Department of Pathology, Northwestern University, Chicago, Illinois. [6]Department of Neurologic Surgery, Northwestern University, Chicago, Illinois. [7]Department of Medicine, Northwestern University, Chicago, Illinois. [8]Colorado State University, Flint Animal Cancer Center, Fort Collins, Colorado. [9]Lyell Immunopharma, Seattle, Washington. [10]Division of Hematology and Oncology, Seattle Children's Hospital, Seattle, Washington. [11]Department of Bone Marrow Transplantation and Cellular Therapy, St. Jude Children's Research Hospital, Memphis, Tennessee. [12]Department of Veterinary Medicine, University of California Davis, Davis, California.

Note: Supplementary data for this article are available at Molecular Cancer Therapeutics Online (http://mct.aacrjournals.org/).

Corresponding Author: Seth M. Pollack, Oncology, Northwestern University, 303 E. Superior St. #3-115, Chicago, IL 60611. E-mail: seth.pollack@northwestern.edu

Mol Cancer Ther 2022;21:999–1009

doi: 10.1158/1535-7163.MCT-21-0726

incidence rates make working with primary canine tumors, treating patient dogs, and adjusting treatment regimens a sustainable choice.

The treatment of naturally occurring canine malignancies with CAR T cells offers the opportunity to tailor comprehensive immunotherapeutic strategies in an immunocompetent host. However, there are significant obstacles including the lack of well-known tumor antigens, specific antibodies, as well as methods and reagents for canine immunology research. Several groups generated canine CAR T cells for canine lymphoma by targeting canine CD20, canine osteosarcoma by targeting HER2, canine glioma by targeting IL13Rα2, and showed promising results in some cases (10–13). However, current canine CAR T-cell production processes differ considerably from most of the human CAR T cells due to the lack of available resources. Therefore, our study aims to broaden the options for canine solid tumor treatment, with CAR T cells that highly resembles the human CAR T-cell products. We also want to deepen the understanding of immune responses after lymphodepletion and CAR T-cell infusion in dogs (10, 11), and thus help establishing canine models for cancer immunotherapy research.

B7-H3 (CD276) is a tumor surface antigen that is broadly expressed in solid tumors and showed promising results as a target by CAR T cells in xenograft mouse models (14–19). MGA271 (enoblituzumab), a human B7-H3–specific antibody was shown to have potent antitumor activity *in vitro* and in xenograft models (20) and safe and effective across several tumor types in humans in a phase I clinical trial (21). The same B7-H3 antibody clone MGA271 was tested in the form of single-chain variable fragment (scFv) in a CAR construct in mouse models and showed promising potential in killing human solid tumors (17–19).

In this study, we confirmed that B7-H3 is expressed on canine tumor cell surfaces, the specificity of MGA271 can be extended to canine B7-H3, and MGA271-based canine CAR T cells can kill canine B7-H3$^+$ tumor cells. We developed methods to produce canine CAR T cell with high efficiency. We designed a treatment plan, including intensive lymphodepletion, that is similar to human treatment and can be applied to client-owned animals. Safety of the product and treatment plan was tested in purpose-bred dogs, while clinical and immune responses were closely monitored. This study will allow treatment studies in client-owned animals aimed at improving future studies of CAR T cells in human malignancies.

Materials and Methods

Cell lines

Human cell lines HEK293, MG63 and canine osteosarcoma cell line D17 were purchased from ATCC. Additional canine osteosarcoma cell lines Moresco, McKinley, and Gracie were kind gifts from Dr. Bernard Seguin. Canine osteosarcoma cell line HMPOS was a kind gift of Prof. Rowan Milner from University of Florida (Gainesville, FL). Retrovirus packaging cell line 293GP-GLV was kindly gifted by Dr. Thomas Blankenstein from Max-Delbrück-Center for Molecular Medicine in Berlin, Germany.

Tumor sample processing

Surgically removed tumors were collected from collaborating veterinary hospitals under patient dog owners' consent. Tumor samples were kept in AQIX RS-I Storage and Transport Media (AQIX) before processing. Upon arrival, part of the tumor sample was fixed in 10% formalin and embedded in paraffin tissue blocks. To prepare single-cell suspensions, tumor specimens were cut into small pieces, and transferred into gentleMACS C tubes (Miltenyi Biotec) with enzymatic cocktail containing type IV collagenase, DNase, and hyaluronidase. The tubes were then placed on the MACSmix tube rotator in the incubator at 37°C for 30 minutes. Tumor pieces were disassociated with the gentleMACS disassociator (Miltenyi Biotec) then pressed through a 70-μm mesh cell strainer. Tumor single-cell suspension samples were cryopreserved until later use.

IHC

Staining was performed on 4-μm-thick formalin-fixed paraffin-embedded (FFPE) sections by using automated staining. After deparaffinization, slides were treated with antigen retrieval (AR) buffer (Diva Decloaker from BioCare Medical or Leica Bond Epitope Retrieval Solution 2) and heated for 15 minutes at 95°C–100°C. Slides were cooled in the AR buffer for 15 minutes at room temperature and then rinsed with deionized water and 1 × TBS with Tween-20. Endogenous peroxidase was blocked using 3% hydrogen peroxide. Protein stabilization and background reduction was done using intelliPATH Background Punisher. Slides were then incubated for 1 hour with primary antibodies against B7-H3 (clone RBT-B7H3) followed by the secondary antibody (PerkinElmer OPAL Polymber HRP Ms Plus Rb) application for 30 minutes. Staining was done either by DAB (3, 3′-diaminobenzidine) or fluorochrome. Tertiary TSA-amplification reagent (PerkinElmer OPAL fluor) for 10 minutes. Antigen stripping was performed by heating with Biocare medical denaturation reagent at room temperature. Slides were imaged with Leica SP8 confocal microscope or scanned by Aperio Scanscope.

Canine CAR constructs

Lentiviral construct pHIV7-MGA271-hu41bbz-tEGFR was gifted by Dr. Michael Jensen. Retrovirus vector pSFG-FRP5-ca28z was provided by Dr. Stephen Gottschalk. A short canine 4-1BB signaling domain gene was synthesized by Integrated DNA technologies (IDT). Fragments of the four final constructs: pSFG-MGA271-ca41bbz-tEGFR, pSFG-MGA271-ca28z-tEGFR, pSFG-FRP5-ca41bbz-tEGFR, and pSFG-FRP5-ca28z-tEGFR were amplified from the constructs and synthesized oligo mentioned above and reassembled by overlap extension PCR. Full-length CAR-tEGFR (truncated EGFR) fragments were digested by restricted enzymes and ligated into the pSFG plasmid. The sequences of all the constructs were confirmed by capillary electrophoresis-based sequencing at the genomics core at Fred Hutch.

Flow cytometry

The following antibodies were used to analyze canine immune marker expression: anti-canine CD3/CD4/CD8 conjugated with FITC/PE/AF647 master mix (clone CA17.2A12/YKIX302.9/YCATE55.9, Bio-Rad), anti-canine CD25-super bright 600 (clone P4A10, Thermo Fisher Scientific), anti-CD62L-PE-Atto594 (clone FMC46, Novus Biologicals), anti-CD94-BV786 (clone HP-309, BD Biosciences). Anti-EGFR-BV711 (clone AY13, BioLegend) was used to detect truncated EGFR on the surface of CAR-transduced cells. Both human and canine B7-H3 were detectable by anti-B7-H3-APC (clone MIH42, BioLegend). After staining, samples were acquired immediately on a BD LSR II or BD symphony or sorted with a BD Aria II. Flow data were analyzed by Flowjo v10.

Generation of GFP$^+$ cell lines

All tumor cell lines used as target in killing assays were transduced with GFP. pRRL-GFP was gifted by Dr. Beverly Torok-Storb and used to generate lentivirus for the transduction of the osteosarcoma cell lines MG63, D17, Moresco, McKinley, and Gracie. GFP$^+$ tumor cells were sorted on a BD Aria II after 7 days in culture.

Lentivirus and retrovirus production

Lentivirus packaging plasmid psPAX2, envelope plasmids pMD2.G encoding VSVg and pHCMV-10A1 were purchased from Addgene. Lentivirus transfer plasmids (pHIV7-MGA271-hu41bbz-tEFGR and pRRL-GFP), packaging and envelope plasmids were transfected into the HEK293 cells with lipofectamine 2000 (Thermo Fisher Scientific) according to the manufacturer's instructions. Media containing plasmids was carefully replaced with new media after 15 hours. Viral supernatant was collected twice at 48 and 72 hours, respectively after transfection. Viral supernatant was filtered by a 0.45 μm filter, used fresh or frozen at −80°C until future use.

Depending on the envelopes tested, two systems were used for the retrovirus production. For VSVg, and 10A1, retrovirus packaging plasmid pUMVC was used (purchased from Addgene). Retroviral transfer plasmid [pSFG-FRP5-ca28z, pMP71-human T-cell receptor (TCR)], packaging and envelope plasmids were transfected into HEK293 cells with lipofectamine 2000. For gibbon ape leukemia virus (GALV) envelope, transfer plasmids were transfected into the packaging cell line 293GP-GLV without packaging and envelope plasmids. The methods for transduction and viral supernatant collection were the same for retrovirus as for lentivirus.

Activation and transduction of canine T cells

Canine blood was collected from healthy donor dogs from the canine facility at Fred Hutchinson Cancer Research Center. peripheral blood mononuclear cells (PBMC) were isolated by Ficoll (GE life sciences). To activate canine T cells, anti-canine CD3 (clone 17.6F9) and anti-canine CD28 (clone 1c6, kind gift from Dr. Rainer Storb from Fred Hutchinson Cancer Research Center) were diluted with PBS and plated in non–tissue culture–treated cell culture wells at concentrations of 5 and 1 μg/mL, respectively. The plates were coated with the antibodies at 4°C overnight, blocked with 2% BSA at room temperature for 30 minutes, and washed with PBS. Canine PBMCs were thawed and seeded at 0.5×10^6/mL in CTL media with 500 IU/mL recombinant human IL2 (rhIL2; Gibco). T cells were transduced twice to ensure a high transduction efficiency. This method is adapted from (22). On day 4, CAR-encoding viral supernatant supplemented with 500 IU/mL rhIL2 and 4 μg/mL protamine sulfate was added into the cell culture for the first transduction. For the second transduction, non–tissue culture–treated cell culture plates or flasks were coated with 25 or 10 μg/mL retronectin (Takara) at 4°C overnight. On the next day, the plates for flasks were blocked with 2% BSA, washed with PBS, and coated with viral supernatant at 4°C overnight. On day 5, the viral supernatant was then removed and cells that were transduced with protamine sulfate were resuspended and added onto the retronectin and virus coated plates or flasks. Cells were counted every 3–4 days and cell concentration was adjusted to $0.5–1 \times 10^6$ cells/mL with CTL media supplemented with 200 IU/mL rhIL2 until day 14. Replication competent retrovirus was tested at Indiana University (Bloomington, IN) by qPCR of the GALV gene. Endotoxin, *Mycoplasma*, and bacterial infection were tested at the quality control lab at the cell production facility at Fred Hutch.

Spheroids killing

GFP^+ target tumor cells were seeded in 96-well ultralow attachment plates (Corning) at 2,000 cells/well. The plates were centrifuged for 10 minutes at 125 g and kept still at 37°C for 2–3 days to allow spheroids to form. Effector cells were added into spheroid containing wells with different E:T ratios (typically 1:1–4:1) as indicated in the texts. The plates were then transferred into an Incucyte S3 live-cell analysis system (Sartorius), images of bright field and GFP were captured every 2 hours for 3 days. Intensity of GFP was analyzed to represent the amount of target cells in the well.

Cryopreservation and thawing of the product

CAR T-cell product from subject 1 was cryopreserved 7 weeks prior to the infusion. According to the dog's weight, $1 \times 10^9/m^2$ autologous CAR T cells were resuspended in 5 mL of heat-inactivated autologous plasma, 4 mL of normosol-R, and 1 mL of DMSO. The 10 mL of cell suspension was mixed well, kept cool, and injected into a cryobag (50 mL, Baxter). The cryobag was transferred to a controlled-rate freezer (CryoMed model 1010) at the Co-operative Center for Excellence in Hematology (CCEH) core at Fred Hutch, and transferred immediately after the freezing process to the liquid nitrogen for storage. On the day of infusion, cryobag was thawed in warm water while having 40 mL of room temperature Normosol-R injected into the bag. Cells were not washed to avoid chances of contamination and infused immediately after thawing.

Safety protocol design

The safety study was approved by Fred Hutchinson Cancer Research Center's Institutional Animal Care and Use Committee, approval number PROTO201900860. Peripheral blood was drawn for CAR T-cell production. On day 4 and day 3, 4 and 3 days prior to the CAR T-cell infusion day (day 0), cyclophosphamide (orally, 400 mg/m^2) and fludarabine (i.v., 10 mg/m^2) were given to the dogs for lymphodepletion. Furosemide (s.c., 400 mg/m^2) was given alongside to prevent potential harm to the kidneys and bladder caused by cyclophosphamide. On day 0, dogs were premedicated with diphenhydramine (i.v., 2 mg/kg) 30–60 minutes prior to cell infusion. CAR T-cell product ($1 \times 10^9/m^2$, >30% transduction efficiency, >70% viability, negative for *Mycoplasma* and bacterial contamination, endotoxin <0.5 EU/mL) was resuspended in 50 mL Normosol-R solution (Hospira) supplemented with 10% heat-inactivated autologous plasma. The cell products were infused slowly through the intravenous catheter over 20 minutes. Cetuximab was given to the subjects between week 6 and week 8 (i.v., 200 mg/m^2).

Blood samples were collected, and complete blood count (CBC) were measured at least once per week throughout the study. Chemistries were measured three times a week for the first week, and once per week thereafter. Bone marrow (BM) and lymph node (LN) aspirate samples were acquired on week 4 and 6 postinfusion, as well as 2 weeks after cetuximab treatment. The following parameters were monitored closely at least once per day for the first 2 weeks and at least three times a week afterward: body temperature, eyes, ears, mucous membranes, skin turgor, petechia, LN palpation, abdominal palpation, stool, vomiting, activity level, behavior, appetite, and pain/distress.

qRT-PCR

RNA from PBMC, LNs, and BM were isolated using RNeasy micro kit (Qiagen). cDNA was synthesized from 500 ng of RNA using superscript IV first-strand synthesis system (Invitrogen). SsoAdvanced Universal SYBR Green Supermix (Bio-Rad) was used to perform real-time PCR on the Applied Biosystems StepOnePlus. All primers were designed using Primer 3 and synthesized by IDT and the sequences are listed as follows, canine GAPDH F': GAGATCCCGCCAACATCAAATGG, R': TACTTCTCATGGTTCACGCCCAT; Human tEGFR F': GGAGAGGGCAGAGGAAGTCT, R': TGGAGGTGCAGTTTTTGAAG. Human tEGFR expression was normalized to internal control canine GAPDH to represent the CAR transgene expression level.

Serum cytokine measurement

Serum samples were collected, aliquoted, and stored at −80°C. All the samples were thawed and analyzed at the same time using the Cytokine/Chemokine/Growth Factor 11-Plex Canine ProcartaPlex Panel 1 kit from Thermo Fisher Scientific. Samples were measured in duplicate, followed by the manufacturer's protocol.

Data availability

The data generated in this study are available upon request from the corresponding author.

Results

B7-H3 is expressed on canine osteosarcoma and other tumors

The expression of B7-H3 molecule on canine tumor surface was analyzed on canine osteosarcoma cell lines, primary canine tumors, and archived FFPE. Because of the high sequence homology between human and canine B7-H3 (Supplementary Fig. S1A), we were able to find cross-reactive anti-human B7-H3 antibodies for canine B7-H3. Flow cytometry results using anti-human B7-H3 antibody (clone MIH42) showed all four canine osteosarcoma cell lines tested (D17, Moresco, McKinley, and Gracie) stained positive for B7-H3 on the cell surface (Supplementary Fig. S1B).

Nine surgically removed canine tumors (one melanoma, six osteosarcoma and two STS) were processed into single-cell suspensions and analyzed by flow cytometry (**Fig. 1A**). As no defined tumor antigen is known to distinguish tumor cells from inflammatory infiltrates and stromal cells for these canine tumors, we analyzed the expression of B7-H3 on $CD45^-$ cells, presumably a considerable fraction of which were tumor cells. Among $CD45^+$ cells, CD11b expression and cell size (forward scatter, side scatter) were used to distinguish lymphocytes from myeloid cells. OSA-1, a splenic

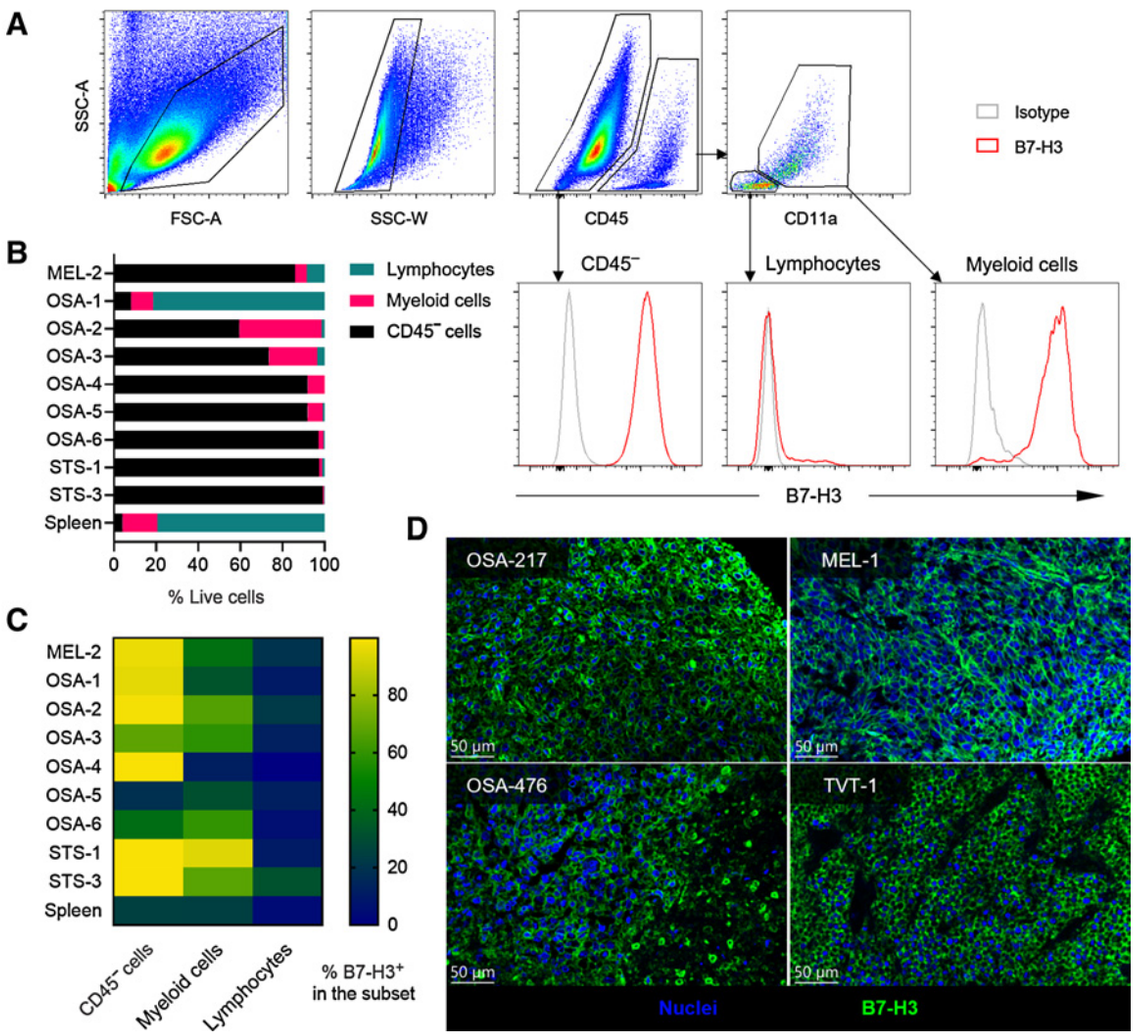

Figure 1.

B7-H3 is expressed on canine solid tumors. **A,** Gating strategy of $CD45^-$ cells, tumor-infiltrating lymphocytes, and myeloid cells on a STS sample (STS-1), and the expression levels of B7-H3. **B,** Summary of the frequencies of $CD45^-$ cells, lymphocytes, and myeloid cells from each sample. Spleen samples were included as a negative control. **C,** Expression level of B7-H3 on different cell subsets from each tumor sample. Tumor cells generally have the highest level of B7-H3, followed by myeloid cells. **D,** Representative IHC results of surface B7-H3 expression on canine osteosarcoma, melanoma (MEL) and TVT. Blue indicates nuclei and green indicates B7-H3 staining.

Table 1. CAR T-cell product characterization.

	Subject 1	Subject 2
Age (yr)/sex	1/M	6/M
Weight (kg)	16	15.4
Infused cells ($\times 10^6$)	641	625
Fresh/frozen	Frozen	Fresh
Formulation	44 mL Normosol-R 5 mL autologous plasma 1 mL DMSO	45 mL Normosol-R 5 mL autologous plasma
Production start ($\times 10^6$)	20	20
Production end ($\times 10^6$)	2,729	6,560
Transduction efficiency	32.9%	47.6%
CD4:CD8	1.77	0.89

metastasis, was comprised of the most immune cells, which could be attributable to the special location of the tumor. The other canine tumor samples had $CD45^+$ immune cell infiltration ranging from 0.8% to 40% (median 8%). Of the infiltrating immune cells, the majority were myeloid cells. The lymphocyte frequencies ranged from 0.2% to 8.4% (median 1%), of all live cells (**Fig. 1B**). The majority of $CD45^-$ cells were positive for B7-H3 (18.7%–99.9%, median 96.9%; **Fig. 1C**). Myeloid cells were also partially positive for B7-H3, but at a significantly lower frequency. Lymphocytes were largely negative for B7-H3. Finally, we analyzed archived primary canine osteosarcoma and other tumor FFPE samples by IHC and found clear tumor cell surface expression of B7-H3 on (6/8) osteosarcoma, (1/2) melanoma samples, and one canine transmissible venereal tumor (TVT; **Fig. 1D**). These data suggest that B7-H3 is indeed expressed on the surface of canine solid tumor cells and may potentially be targeted by B7-H3 CAR T cells.

Activation and transduction of canine PBMCs

To activate and virally transduce CAR-expressing canine T cells, we developed canine T-cell stimulation protocols using anti-canine CD3 (clone 17.6F9; ref. 23) in combination with anti-canine CD28 (clone 1c6; ref. 24) that induced strong proliferation of T cells *in vitro*. Indeed, following anti-canine CD3/CD28 stimulation, canine T cells expanded more than 100 folds, and up to 300 folds with supplemental rhIL2 and FBS (Supplementary Fig. S2A; **Table 1**).

Using a gamma retroviral vector, we tested the commonly used envelopes VSVg, murine leukemia virus envelope 10A1, and GALV envelope but found that GALV was the only envelope that resulted in a satisfactory transduction efficiency (Supplementary Fig. S2B). With further optimization, the transduction efficiencies of canine T cells were consistently over 30% up to 80% without the need of sorting or coculture with specific antigen or feeder cells.

B7-H3 CAR derived from human antibody recognize and kill canine tumor spheroids

A tEGFR consisting of the extracellular domain and transmembrane domain of the human EGFR was added to the canine HER2 CAR construct pSFG-FRP5-caCD28z (12) to better trace the CAR T cells, as surface $EGFR^+$ T cells would be CAR-transduced cells. Truncated EGFR also serves as a safety measure because $EGFR^+$ CAR T cells can be depleted *in vivo* by cetuximab (25, 26). The MGA271 scFv was synthesized according to the online sequence of the humanized B7-H3 antibody published by Macrogenics (Patent no. US 10,730,945 B2) and cloned into the CAR constructs. The four constructs tested in the study are illustrated in **Fig. 2A**. Signaling domains of CD28, 4-1BB, and CD3 used in this study are all canine versions.

MGA271-CD28z, MGA271-41bbz, FRP5-CD28z, and FRP5-41bbz CARs were transduced into canine T cells. Untransduced and TCR-transduced canine T cells were activated and cultured at the same time to serve as negative controls (**Fig. 2B**). We subsequently sorted $EGFR^+$ T cells, cocultured with GFP^+ canine osteosarcoma spheroids and analyzed the killing dynamics to determine whether MGA271 CAR was able to recognize canine B7-H3. Comparing with negative control T cells, MGA271 CAR T cells can efficiently eliminate tumor spheroids formed by B7-$H3^+$ osteosarcoma cell lines Moresco, D17, McKinley, and Gracie (**Fig. 2C** and **D**; Supplementary Fig. S3A). B7-H3–negative canine osteosarcoma HMPOS was not targeted by MGA271 CAR T cells (Supplementary Fig. S3B; ref. 27). Killing of the Moresco spheroids by the MGA271 CARs was faster and more thorough compared with HER2-targeting FRP5 CARs (**Fig. 2C** and **D**), which could potentially be attributable to the tumor surface B7-H3 and HER2 molecule expression levels and affinities of the two scFvs to their respective ligands. No statistically significant difference in killing dynamics was observed between different signal 2 signaling domains of the same scFv CARs.

These results showed canine MGA271 CAR T cells can kill B7-H3–positive tumor cells *in vitro*, and hence confirmed the specificity of MGA271 CAR to canine B7-H3. MGA271-41bbz was selected for further analyses of *in vivo* safety due to its high *in vitro* cytotoxicity.

Clinical manifestations after lymphodepletion, CAR T-cell infusion, and cetuximab administration

To evaluate the safety of B7-H3–targeting canine CAR T cells in a clinically relevant context, we designed an intensive lymphodepleting conditioning regimen for healthy canine subjects that included cyclophosphamide (400 mg/m^2) and fludarabine (10 mg/m^2) on days 4 and 3 (**Fig. 3A**). Cryopreserved (subject 1) or fresh (subject 2) CAR T cells were infused at a dose of 1×10^9 cells/m^2 (**Table 1**). Cetuximab was administered 6 to 8 weeks after CAR T-cell transfer to test the safety albeit in a cell population that may be undetectable, as *in vivo* CAR T-cell depletion may be required in future patient dog treatment. Clinical manifestations including body temperature, eyes, ears, mucous membranes, skin turgor, petechia, LN palpation, abdominal palpation, stool, vomiting, activity level, behavior, appetite and pain/distress and immune responses were closely monitored throughout the study.

Lymphodepletion with cyclophosphamide and fludarabine and B7-H3 CAR T-cell infusion were well tolerated. No abnormalities were observed in subject 1 after lymphodepletion and CAR T-cell infusion. Subject 2 experienced fever, skin dehydration, and anorexia (**Table 2**). The highest body temperature was 40.7°C, observed one day after CAR T-cell infusion. All symptoms were manageable by veterinarians and returned to normal within 3 weeks after infusion.

As expected, following lymphodepleting chemotherapy, CBC showed that lymphocyte counts decreased to a nadir around day 0 (CAR T-cell infusion day) continuing until approximately 4 days after completion of lymphodepleting conditioning in both subjects (**Fig. 3B**), with the lowest count of 400/μL for subject 1 and 60/μL for subject 2. Lymphocyte counts remained low (<1,000/μL) for another 4 days for subject 1 and 8 days for subject 2, and gradually returned to the baseline level with occasional fluctuation. Other parameters including white blood cells, absolute neutrophil counts, and platelets followed similar trend (Supplementary Fig. S4).

Cetuximab treatment on day 58 for subject 1 and day 44 for subject 2 did not have clear impact on lymphocyte counts. Subject 1 developed skin, ear, and oral lesions on day 67, 9 days after cetuximab injection

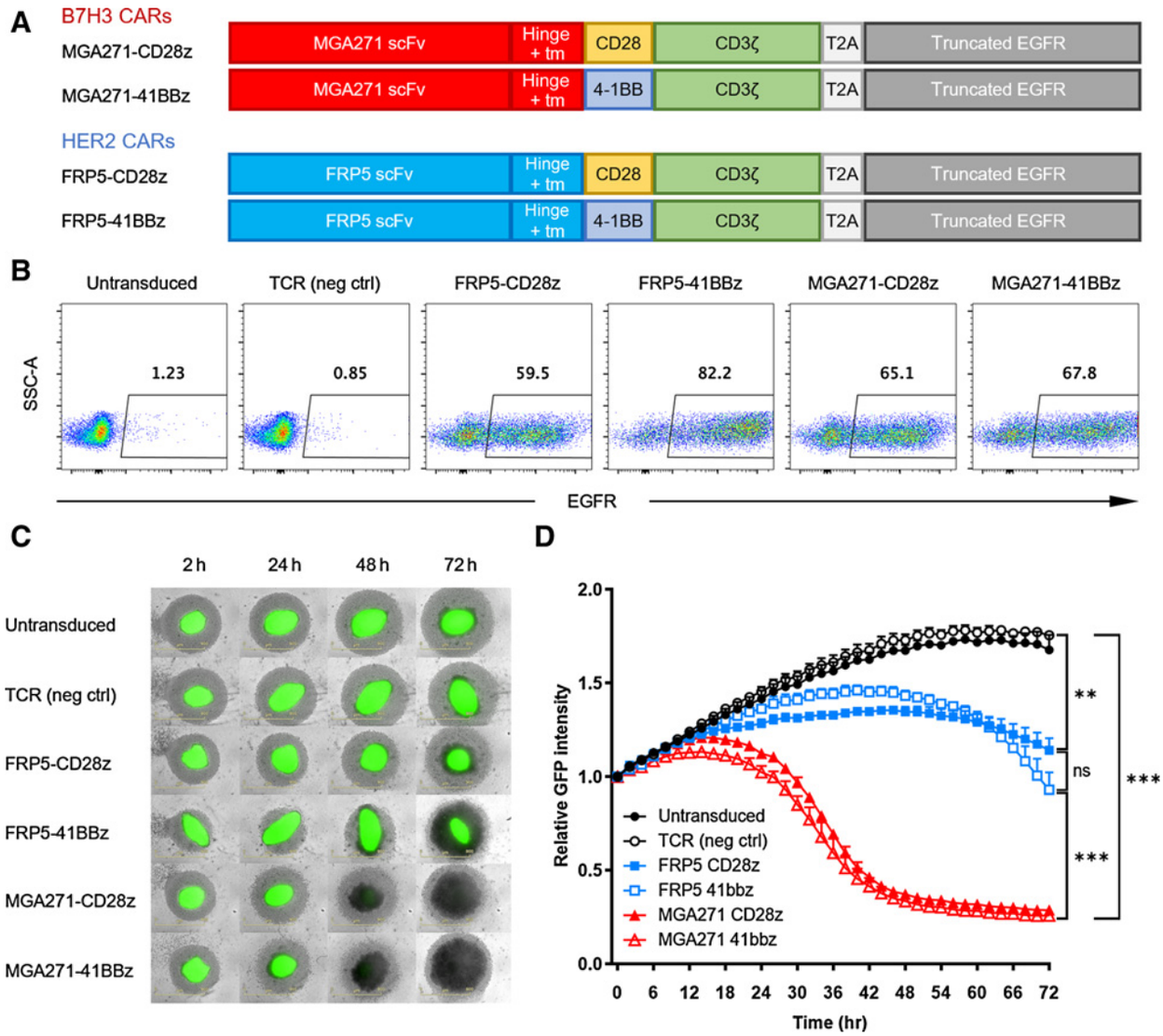

Figure 2.

Canine MGA271 CAR T cells are efficient at killing canine osteosarcoma spheroids. **A,** Four CAR constructs were used in this study. Each construct consists of a scFv, a hinge, a transmembrane domain (tm), a canine costimulatory signaling domain, a canine CD3 signaling domain, T2A, and a truncated human EGFR sequence. **B,** Flow plots of day 14 transduction efficiencies of different constructs by EGFR staining. **C,** Longitudinal images of GFP-transduced canine osteosarcoma Moresco spheroids (green) cocultured with sorted canine CAR T cells (light gray) at E:T ratio of 2:1. Untransduced and TCR-transduced canine cells were used as negative controls. All conditions were measured in triplicates. **D,** Summary of relative GFP intensity of Moresco spheroids cocultured with different T cells. Graph shows mean ± SD. Samples were measured in triplicate. Statistical analysis was performed using the multiple group comparison Holm-Šídák test; ***, $P < 0.001$; **, $P < 0.01$; ns, not significant.

(**Table 2**). It is unclear whether it was delayed reaction to cetuximab, as these lesions are not uncommon for canines and could potentially be allergic reaction to environmental factors like insect bites. The symptoms were alleviated by diphenhydramine treatment and resolved on day 71. Subject 2 had no side effects after cetuximab injection.

Persistence of B7-H3 CAR T cells in purpose-bred dogs

The frequency of EGFR$^+$ cells from subject 1 peaked on day 2 comprising about 0.1% of all peripheral lymphocytes (**Fig. 3B**). Subject 2 reached a higher peak frequency of EGFR$^+$ T cell in the periphery. On day 4, 3.4% of the peripheral lymphocytes were CAR T cells. EGFR$^+$ CAR T cells became undetectable by flow cytometry roughly a week after the infusion in both subjects. Phenotypical analysis of the day 4 EGFR$^+$ T cells from the periphery lacked CD25 expression (**Fig. 3C**), and day 4 postinfusion CAR T cells from the blood had an increased frequency of CD62 L expression compared with preinfusion product. The CD4:CD8 ratio remained similar to the preinfusion ratio. B7-H3 CAR T cells were not detectable by flow cytometry at later timepoints in either subjects or in the BM and LN aspirates.

To increase the sensitivity of CAR T-cell detection and rule out the protein expression modulation of the CAR T cells, we performed qRT-PCR to detect the transgene expression in the cells from

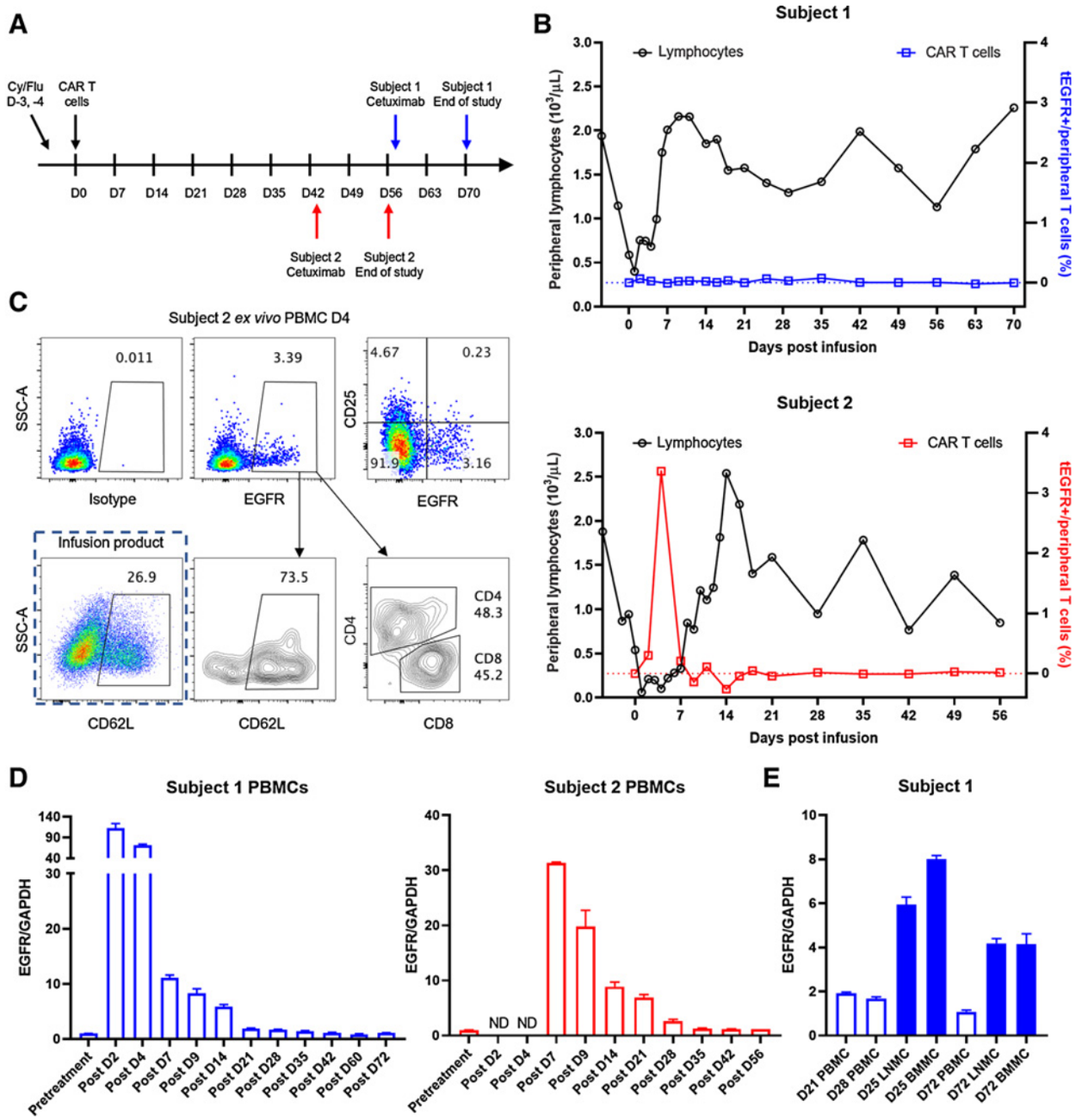

Figure 3.

Limited persistence of CAR T cells in the periphery of healthy dogs. **A,** Timeline for lymphodepletion, CAR T cell, cetuximab treatments, and sample collection. Doses for drugs and biologicals: cyclophosphamide (Cy) 400 mg/m^2, fludarabine (Flu) 10 mg/m^2, CAR T cells 1×10^9/m^2, cetuximab 200 mg/m^2. **B,** Peripheral lymphocyte counts (left axis) and frequency of EGFR$^+$ CAR T cells in the blood (right axis) of the two subjects following the treatment plan. Values shown in the plots are EGFR frequencies subtracted by isotype frequencies from the same sample. **C,** Flow plots showing day 4 *ex vivo* EGFR staining from subject 2, phenotype of EGFR$^+$ cells, and CD62 L expression of infusion product. **D,** qRT-PCR was performed on PBMCs from canine subject 1 and 2 pre- and post- CAR-T treatment (left and middle). Transgenic truncated human EGFR expression was normalized to internal control GAPDH to reflect CAR T-cell frequencies. **E,** Additional mononuclear cell samples from LN and BM from subject 1 was analyzed for CAR T-cell persistence. The samples were analyzed in triplicate, error bars indicate SD. ND, not done (due to the lack of cryopreserved samples).

periphery, LN and BM samples. By qRT-PCR, transgenic tEGFR can be detected in the PBMCs at least till day 14 for subject 1 and day 28 for subject 2 (**Fig. 3D**). Because of the lack of cryopreserved samples, mononuclear cells from LNs and BM were analyzed only for subject 1. Interestingly, comparing with PBMCs, LNMCs, and BMMCs contained more transgenic CAR T cells on both day 25 and day 72 (**Fig. 3E**), suggesting canine CAR T cells may preferably home to LNs and BM in healthy dogs.

Table 2. Adverse events.

Symptoms	Subject	Days	Interventions
Neutropenia (<2,900/μL)	1	D0 to D7	Enrofloxacin
	2	D5 to D9	Gentamycin, Vancomycin, Enrofloxacin
Lymphocytopenia (<400/μL)	2	D1 to D7	None
Thrombocytopenia (<150,000/μL)	1	D1 to D7	None
	2	D1 to D14	Platelet-rich plasma
Elevated liver enzymes	1	D0–D2 to D4–D14	None
	2	D0–D2 to D21–D42	None
Fever (>39.5°C)	2	D1 to D6, D10	Acetaminophen
Skin dehydration	2	D3 to D11	Lactated ringers
Anorexia (including partial)	2	D4, D6, D7, D10, D11, D18	Capromorelin
Skin, ear, and oral lesions	1	D67 to D71 (9–13 days after cetuximab injection)	Diphenhydramine

Serum chemistry and cytokine change

Blood chemistry panels were run routinely on the two subjects throughout the treatment. The panel include the following parameters: serum glucose, blood urea nitrogen, creatinine, sodium, potassium, Na/K ratio, chloride, carbon dioxide, anion gap, calcium, phosphorus, osmolality, total protein, albumin, globulin, Alb/Glob ratio, bilirubin, alkaline phosphatase (ALP), Gamma-glutamyl Transferase (GGT), alanine aminotransferase (ALT), aspartate aminotransferase (AST), Creatine kinase, Cholesterol, Amylase, and Lipase. Elevations of serum ALP and ALT levels was observed after lymphodepletion and/or CAR T-cell infusion (**Fig. 4A**; **Table 2**). ALP levels peaked on day 2 after CAR T-cell infusion and gradually returned to normal (normal range: 9–68 U/L). Subject 2 had a more prominent increase of ALP and ALT postinfusion, with peak values of 324 and 190 U/L, respectively. Peak ALP level in subject 2 was in the 3-fold to 5-fold of upper limit of the normal range (ULN), grade 2 toxicity according to the Veterinary Co-operative Oncology Group – Common Terminology Criteria for Adverse Events (28). No clinical manifestation of liver dysfunction was seen. Serum AST (**Fig. 4A**) and bilirubin (≤0.1 mg/dL, normal range 0–0.5 mg/dL) remained normal. We confirmed that hepatocytes lacked significant expression of B7-H3 in four healthy canine livers (Supplementary Fig. S5). All the other parameters remained normal till the end of the study.

In both subjects, monocyte chemoattractant protein-1 (MCP-1/CCL2) concentration increased after lymphodepletion, to the peak concentration 458 and 4,079 pg/mL, respectively and decreased after day 4 (**Fig. 4B**). Concentrations of other serum cytokines including IFNγ, TNFα, IL2, IL6, IL8, IL10 increased after CAR T-cell infusion, peaked at approximately week 2 after infusion, and slowly decreased until week 8. Cytokine release syndrome (CRS)-related cytokine IL6 had the peak concentrations of 263 pg/mL for subject 1 and 127 pg/mL for subject 2.

Subject 1 had drastic increase of cytokine concentration from day 60 to the end of study, which coincided with cetuximab injection (day 58) and the development of skin, ear, and oral lesion. No clear increase of cytokine concentration was observed in subject 2 after cetuximab administration. Subject 1 had a full recovery on day 72. Both subjects were tested normal by routine CBC and chemistry test and were released by the end of the study.

Discussion

In this study, we demonstrated the safety and feasibility of canine CAR T cells targeting B7-H3 to be used for the treatment of dogs with naturally occurring cancers and as a model for human T-cell therapy. Despite the relatively small number of tumor samples, we found consistent B7-H3 expression on different canine tumor types confirming data from several recent studies that have also suggested its importance and potential as a broad therapeutic target (27).

In human patients with cancer, high expression level of B7-H3 is associated with poor prognosis in some malignancies (29–31). Although the receptor and its downstream signaling cascade have not been identified, B7-H3 has an inhibitory effect on T-cell functionality *in vitro* and in murine models (32). Therefore, by eliminating B7-H3$^+$ cells, patients' endogenous immune responses may be stimulated in addition to the direct B7-H3–specific CAR T cell–mediated killing.

In previous canine CAR T-cell studies, Phytohaemagglutinin (PHA) and/or artificial antigen-presenting cells stimulations were often used for T-cell activation instead of anti-CD3/CD28 that is commonly used for human CAR T-cell production. These two activation methods can lead to different T-cell behaviors (33), and therefore influence the representativeness of the model. Our CAR T-cell production method uses agonist antibodies specific for canine CD3ε and CD28 for T-cell activation, which closely resembles human CAR T-cell production and does not require additional feeder cell stimulation for consistently high level of expansion and transduction efficiency. Therefore, this method is suitable for clinical trial for client-owed dogs and an ideal animal model for human cancer immunotherapy research.

Neither subject had any concerning adverse events after receiving the intensive lymphodepletion regimen and one of the highest doses of CAR T cells tested in human. While this safety data is sufficient to begin testing the treatment regimen in client owned animals suffering from cancer, future studies should monitor animals closely to be sure there are not additional toxicities beyond what was observed. Because B7-H3 is generally not highly expressed by healthy tissues, the expansion and persistence of CAR T cells were not as well in healthy dogs as what we would expect in patient dogs. In future trials, *in vivo* expansion of infused cells could potentially lead to CRS and tumor lysis syndrome, and a dose-escalation trial is a plausible option. Mild hepatotoxicity is a common finding in human CAR T-cell trials. Given that no strong expression was seen in hepatocytes from healthy liver samples, this is likely due either to lymphodepleting chemotherapy or metabolism of infused cells. Regardless, this could be an important potential cause of toxicity that needs to be watched closely in future studies.

Similar to human CAR T cells trials, the canine subjects also saw increased concentrations of serum cytokines including IFNγ, IL6,

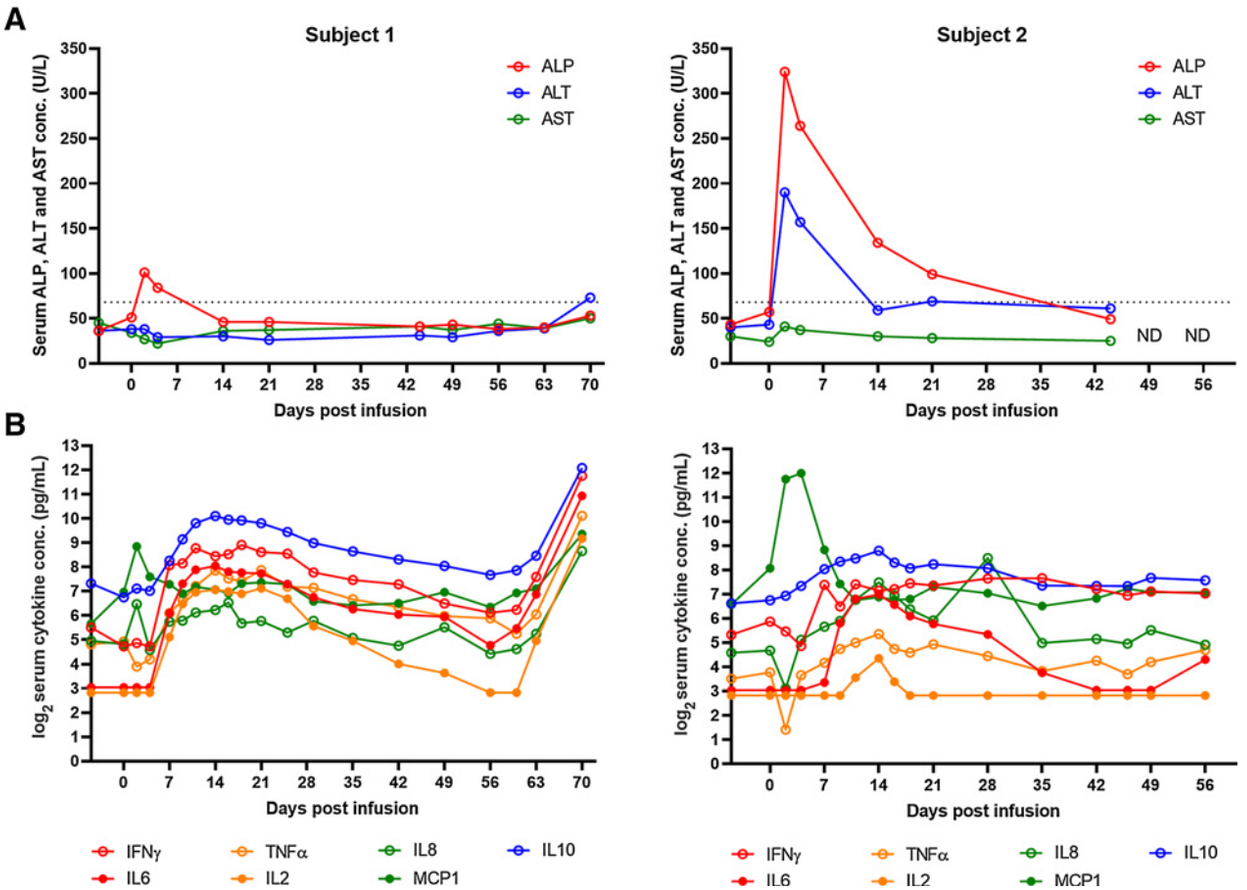

Figure 4.

Treatment plan for healthy dogs, post-treatment clinical and immunologic responses. **A,** Serum ALP and ALT level change in the 2 healthy dog subjects following the treatments. ND, not done. **B,** Serum cytokine level change following the treatments. Cytokine concentration was measured in duplicates, data points indicate the mean values.

TNFα, IL2, IL8, MCP1, and IL10 after lymphodepletion and CAR T-cell infusion (34–36). The dynamic of serum MCP1 concentration change is earlier than the other cytokines, suggesting MCP1 was induced by lymphodepletion rather than CAR T-cell infusion, which is consistent with human study showing that high MCP1 concentration at the time of CAR T-cell infusion correlates with better outcome (37). This observation further supports the relevance of the canine model to clinical study of human CAR T cells (38). Our results in healthy dogs also provide baseline comparison for future patient dog treatment to distinguish immune response against immunotherapy from that against tumor cells.

In summary, we confirmed *in vitro* that canine MGA271 CAR T cells could potentially be an effective treatment for canine solid tumors. We established a canine CAR T-cell production protocol and designed a treatment plan that closely resemble that of human CAR T cells. The lymphodepletion and MGA271 CAR T-cell treatment regimen was shown to be safe. Our model provides a highly feasible and scientifically relevant model for solid tumor targeting CAR T-cell research.

Authors' Disclosures

B.J. Hayes reports grants from NIH NIDDK during the conduct of the study. A.I. Salter reports personal fees from Lyell Immunopharma outside the submitted work; in addition, A.I. Salter has a patent for Chimeric receptor proteins and uses thereof issued, licensed, and with royalties paid from Lyell Immunopharma. S.R. Riddell reports grants and personal fees from Lyell Immunopharma and Juno/Bristol Myers Squibb, and personal fees from Adaptive Biotechnologies outside the submitted work. S. Gottschalk reports personal fees from TESSA Therapeutics, Immatics, Catamaran Bio, TIDAL, and Nektar Therapeutics outside the submitted work; in addition, S. Gottschalk has a patent for B7-H3 Chimeric Antigen Receptors pending. S.M. Pollack reports personal fees from T-knife, Deciphera, AAdi, Epizyme, Bayer, Apexigen, GSK, and Springworks; and grants and personal fees from Obsidian outside the submitted work. No disclosures were reported by the other authors.

Authors' Contributions

S. Zhang: Conceptualization, formal analysis, investigation, visualization, methodology, writing–original draft, writing–review and editing. **R.G. Black:** Data curation, investigation, visualization, writing–review and editing. **K. Kohli:** Writing–review and editing. **B.J. Hayes:** Conceptualization, resources, writing–original draft, writing–review and editing. **C. Miller:** Methodology, writing–original draft, writing–review and editing. **A. Koehne:** Conceptualization, investigation, writing–review and editing. **B.A. Schroeder:** Investigation, writing–original draft, writing–review and editing. **K. Abrams:** Conceptualization, investigation, writing–original draft, writing–review and editing. **B.C. Schulte:** Writing–original draft, writing–review and editing. **B.A. Alexiev:** Investigation. **A.B. Heimberger:** Writing–original draft, writing–review and editing. **A. Zhang:** Data curation, investigation, methodology, writing–original draft, writing–review and editing. **W. Jing:** Validation, investigation, visualization, methodology, writing–original draft, writing–review and editing. **J.C.K. Ng:** Validation, investigation, visualization, writing–original draft, writing–review and editing. **H. Shinglot:** Validation, investigation, visualization,

methodology, writing–original draft, writing–review and editing. **B. Seguin:** Resources, writing–original draft, writing–review and editing. **A.I. Salter:** Resources, data curation, writing–review and editing. **S.R. Riddell:** Supervision, writing–original draft, writing–review and editing. **M.C. Jensen:** Resources, supervision, writing–review and editing. **S. Gottschalk:** Resources, data curation, writing–review and editing. **P.F. Moore:** Resources, writing–original draft, writing–review and editing. **B. Torok-Storb:** Resources, writing–original draft. **S.M. Pollack:** Conceptualization, resources, data curation, formal analysis, supervision, funding acquisition, investigation, writing–original draft, project administration, writing–review and editing.

Acknowledgments

Funding for this study came from NCI R01CA244872, the Alliance for Cancer Gene Therapy, the Gilman Sarcoma Foundation, and CA180380. S.M. Pollack was also supported by R01CA244872, CA180380, and a grant from the V Foundation.

We thank our veterinarian collaborators Dr. Jim Perry from CASTR Alliance, Dr.Chelsea Tripp from Bridge Animal Referral Center, Drs. Kevin Choy and Akiko Koshino from Blue Pearl for providing us with canine tumor samples and insights into the project.

We thank Dr. Kenneth Cornetta and the National Gene Vector Biorepository (NGVB) for the help with the RCR test.

We thank David Yadock from the CCEH - Hematopoietic Cell Procurement and Processing Services for the help with cell cryopreservation.

The costs of publication of this article were defrayed in part by the payment of page charges. This article must therefore be hereby marked *advertisement* in accordance with 18 U.S.C. Section 1734 solely to indicate this fact.

Received August 28, 2021; revised January 31, 2022; accepted March 31, 2022; published first April 11, 2022.

References

1. Martinez M, Moon EK. CAR T cells for solid tumors: new strategies for finding, infiltrating, and surviving in the tumor microenvironment. Front Immunol 2019;10:128.
2. Hegde M, Joseph SK, Pashankar F, Derenzo C, Sanber K, Navai S, et al. Tumor response and endogenous immune reactivity after administration of HER2 CAR T cells in a child with metastatic rhabdomyosarcoma. Nat Commun 2020; 11:3549.
3. Navai SA, DeRenzo C, Joseph S, Sanber K, Byrd TT, Zhang H, et al. Administration of HER2-CAR T cells after lymphodepletion safely improves T cell expansion and induces clinical responses in patients with advanced sarcomas [abstract]. In: Proceedings of the American Association for Cancer Research Annual Meeting 2019; 2019 Mar 29–Apr 3; Atlanta, GA. Philadelphia (PA): AACR; Cancer Res 2019;79(13 Suppl):Abstract nr LB-147.
4. Morgan RA, Yang JC, Kitano M, Dudley ME, Laurencot CM, Rosenberg SA. Case report of a serious adverse event following the administration of T cells transduced with a chimeric antigen receptor recognizing ERBB2. Mol Ther 2010;18:843–51.
5. Richman SA, Nunez-Cruz S, Moghimi B, Li LZ, Gershenson ZT, Mourelatos Z, et al. High-affinity GD2-specific CAR T cells induce fatal encephalitis in a preclinical neuroblastoma model. Cancer Immunol Res 2018;6:36–46.
6. Paoloni M, Davis S, Lana S, Withrow S, Sangiorgi L, Picci P, et al. Canine tumor cross-species genomics uncovers targets linked to osteosarcoma progression. BMC Genomics 2009;10:625.
7. Gardner HL, Sivaprakasam K, Briones N, Zismann V, Perdigones N, Drenner K, et al. Canine osteosarcoma genome sequencing identifies recurrent mutations in DMD and the histone methyltransferase gene SETD2. Commun Biol 2019;2:266.
8. Dobson JM. Breed-predispositions to cancer in pedigree dogs. ISRN Vet Sci 2013;2013:941275.
9. Mason NJ. Comparative immunology and immunotherapy of canine osteosarcoma. Adv Exp Med Biol 2020;1258:199–221.
10. Panjwani MK, Smith JB, Schutsky K, Gnanandarajah J, O'connor CM, Powell DJ, et al. Feasibility and safety of RNA-transfected CD20-specific chimeric antigen receptor T cells in dogs with spontaneous B cell lymphoma. Mol Ther 2016;24: 1602–14.
11. Panjwani MK, Atherton MJ, Maloneyhuss MA, Haran KP, Xiong A, Gupta M, et al. Establishing a model system for evaluating CAR T cell therapy using dogs with spontaneous diffuse large B cell lymphoma. Oncoimmunology 2020;9: 1676615.
12. Mata M, Vera JF, Gerken C, Rooney CM, Miller T, Pfent C, et al. Toward immunotherapy with redirected T cells in a large animal model: ex vivo activation, expansion, and genetic modification of canine T cells. J Immunother 2014;37:407–15.
13. Yin Y, Boesteanu AC, Binder ZA, Xu C, Reid RA, Rodriguez JL, et al. Checkpoint blockade reverses anergy in IL-13Ralpha2 humanized scFv-Based CAR T cells to treat murine and canine gliomas. Mol Ther Oncolytics 2018;11:20–38.
14. Zhang Z, Jiang C, Liu Z, Yang M, Tang X, Wang Y, et al. B7-H3-Targeted CAR-T cells exhibit potent antitumor effects on hematologic and solid tumors. Mol Ther Oncolytics 2020;17:180–9.
15. Tang X, Zhao S, Zhang Y, Wang Y, Zhang Z, Yang M, et al. B7-H3 as a Novel CAR-T therapeutic target for glioblastoma. Mol Ther Oncolytics 2019;14: 279–87.
16. Theruvath J, Sotillo E, Mount CW, Graef CM, Delaidelli A, Heitzeneder S, et al. Locoregionally administered B7-H3-targeted CAR T cells for treatment of atypical teratoid/rhabdoid tumors. Nat Med 2020;26:712–9.
17. Majzner RG, Theruvath JL, Nellan A, Heitzeneder S, Cui Y, Mount CW, et al. CAR T Cells Targeting B7-H3, a Pan-cancer antigen, demonstrate potent preclinical activity against pediatric solid tumors and brain tumors. Clin Cancer Res 2019;25:2560–74.
18. Nguyen P, Okeke E, Clay M, Haydar D, Justice J, O'reilly C, et al. Route of 41BB/41BBL costimulation determines effector function of B7-H3-CAR.CD28zeta T cells. Mol Ther Oncolytics 2020;18:202–14.
19. Talbot LJ, Chabot A, Funk A, Nguyen P, Wagner J, Ross A, et al. A novel orthotopic implantation technique for osteosarcoma produces spontaneous metastases and illustrates dose-dependent efficacy of B7-H3-CAR T cells. Front Immunol 2021;12:691741.
20. Loo D, Alderson RF, Chen FZ, Huang L, Zhang W, Gorlatov S, et al. Development of an Fc-enhanced anti-B7-H3 monoclonal antibody with potent antitumor activity. Clin Cancer Res 2012;18:3834–45.
21. Powderly J, Cote G, Flaherty K, Szmulewitz RZ, Ribas A, Weber J, et al. Interim results of an ongoing Phase I, dose escalation study of MGA271 (Fc-optimized humanized anti-B7-H3 monoclonal antibody) in patients with refractory B7-H3-expressing neoplasms or neoplasms whose vasculature expresses B7-H3. J Immunother Cancer 2015;3:O8.
22. Poncette L, Chen X, Lorenz FKM, Blankenstein T. Effective NY-ESO-1-specific MHC II-restricted T cell receptors from antigen-negative hosts enhance tumor regression. J Clin Invest 2019;129:324–35.
23. Georges GE, Storb R, Brunvand MW, Kiem H-P, Moore PF, Malik P, et al. Canine T cells transduced with a herpes simplex virus thymidine kinase gene: a model to study effects on engraftment and control of graft-versus-host disease. Transplantation 1998;66:540–4.
24. Graves SS, Stone DM, Loretz C, Peterson LJ, Lesnikova M, Hwang B, et al. Antagonistic and agonistic anti-canine CD28 monoclonal antibodies: tools for allogeneic transplantation. Transplantation 2011;91:833–40.
25. Wang X, Chang W-C, Wong CW, Colcher D, Sherman M, Ostberg JR, et al. A transgene-encoded cell surface polypeptide for selection, *in vivo* tracking, and ablation of engineered cells. Blood 2011;118:1255–63.
26. Paszkiewicz PJ, Fräßle SP, Srivastava S, Sommermeyer D, Hudecek M, Drexler I, et al. Targeted antibody-mediated depletion of murine CD19 CAR T cells permanently reverses B cell aplasia. J Clin Invest 2016;126:4262–72.
27. Cascio MJ, Whitley EM, Sahay B, Cortes-Hinojosa G, Chang L-J, Cowart J, et al. Canine osteosarcoma checkpoint expression correlates with metastasis and T-cell infiltrate. Vet Immunol Immunopathol 2021;232:110169.
28. Leblanc AK, Atherton M, Bentley RT, Boudreau CE, Burton JH, Curran KM, et al. Veterinary Cooperative Oncology Group-common terminology criteria for adverse events (VCOG-CTCAE v2) following investigational therapy in dogs and cats. Vet Comp Oncol 2021;19:311–52.
29. Mceachron TA, Triche TJ, Sorenson L, Parham DM, Carpten JD. Profiling targetable immune checkpoints in osteosarcoma. Oncoimmunology 2018;7: e1475873.
30. Wang J, Chong KK, Nakamura Y, Nguyen L, Huang SK, Kuo C, et al. B7-H3 associated with tumor progression and epigenetic regulatory activity in cutaneous melanoma. J Invest Dermatol 2013;133:2050–8.

31. Dong P, Xiong Y, Yue J, Hanley SJB, Watari H. B7H3 as a promoter of metastasis and promising therapeutic target. Front Oncol 2018;8:264.
32. Lee Y-H, Martin-Orozco N, Zheng P, Li J, Zhang P, Tan H, et al. Inhibition of the B7-H3 immune checkpoint limits tumor growth by enhancing cytotoxic lymphocyte function. Cell Res 2017;27:1034–45.
33. Duarte RF, Chen FE, Lowdell MW, Potter MN, Lamana ML, Prentice HG, et al. Functional impairment of human T-lymphocytes following PHA-induced expansion and retroviral transduction: implications for gene therapy. Gene Ther 2002;9:1359–68.
34. Grupp SA, Kalos M, Barrett D, Aplenc R, Porter DL, Rheingold SR, et al. Chimeric antigen receptor-modified T cells for acute lymphoid leukemia. N Engl J Med 2013;368:1509–18.
35. Kalos M, Levine BL, Porter DL, Katz S, Grupp SA, Bagg A, et al. T cells with chimeric antigen receptors have potent antitumor effects and can establish memory in patients with advanced leukemia. Sci Transl Med 2011;3:95ra73.
36. Wang X, Popplewell LL, Wagner JR, Naranjo A, Blanchard MS, Mott MR, et al. Phase 1 studies of central memory-derived CD19 CAR T-cell therapy following autologous HSCT in patients with B-cell NHL. Blood 2016;127:2980–90.
37. Hirayama AV, Gauthier J, Hay KA, Voutsinas JM, Wu Q, Gooley T, et al. The response to lymphodepletion impacts PFS in patients with aggressive non-Hodgkin lymphoma treated with CD19 CAR T cells. Blood 2019;133:1876–87.
38. Kohli K, Yao L, Nowicki TS, Zhang S, Black RG, Schroeder BA, et al. IL-15 mediated expansion of rare durable memory T cells following adoptive cellular therapy. J Immunother Cancer 2021;9:e002232.